



Full Length Article

Understanding the structural changes on Fe₂O₃/Al₂O₃ oxygen carriers under chemical looping gasification conditions

Iván Samprón, Francisco García-Labiano, María T. Izquierdo, Luis F. de Diego*

Instituto de Carboquímica, Consejo Superior de Investigaciones Científicas (ICB-CSIC), C/ Miguel Luesma Castán, 4. 50018 Zaragoza, Spain

ABSTRACT

Chemical Looping Gasification (CLG) has emerged recently as a promising technology for producing non N₂-diluted syngas without the need for an external power supply or the expensive use of pure O₂. Many studies have focused on development of oxygen carriers since they are considered a crucial factor in CLG processes. Fe₂O₃/Al₂O₃ (FeAl) oxygen carriers have been proposed due to previous experience in Chemical Looping Combustion (CLC). However, the aggressive conditions of gasification cause a decrease in the mechanical stability of the particles, which can be a challenge for their use in CLG. In this work, the operating conditions and Fe-content required to maintain the particle integrity of oxygen carrier particles during redox cycles in both CLC and CLG operations were determined. Long-term tests, consisting of 300 redox cycles, were conducted in a TGA to simulate the operation in a continuous unit and the results were compared with attrition data obtained from a 1.5 kW_{th} CLG unit. Three oxygen carriers with varying Fe₂O₃-content (10, 20 and 25 wt%) were used, and three different solid conversions (0–25 %, 75–100 % and 0–100 %) were performed to emulate CLC or CLG atmospheres at three temperatures (850 °C, 900 °C and 950 °C). The evolution of the microstructure of particles was analyzed using a scanning electron microscope (SEM) and it was found that the lower the Fe₂O₃ content in the particles, the greater their stability in redox cycles, an increase in the reaction temperature led to a more rapid degradation of the oxygen carrier particles, and the solid conversion variation and degree of reduction/oxidation during redox cycles strongly influenced the evolution of the mechanical stability of the oxygen carrier particles.

1. Introduction

Gasification technologies have been used for many years to generate syngas that can be used either for power and heat generation or for the production of chemicals [1]. Various gasification processes have been developed, which mainly differ in the way of producing the heat needed for endothermic gasification reactions. Thus, heat can be produced by combustion of part of fuel inside of the gasification reactor using air, but the use of air causes dilution by N₂ of the syngas. The use of pure oxygen avoids dilution with N₂ but implies the high cost of the air separation unit (ASU). In dual fluidized bed (DFB) gasification, the combustion of part of fuel takes place in a separated reactor (combustor) and the generated heat is transported by an inert solid to the gasifier, but CO₂ is emitted in the combustor and high concentrations of tar are generated in the gasifier, which cause corrosion on the reactor walls and on the pipes downstream of the gasifier. Based on DFB, Chemical Looping Gasification (CLG) is a promising technology that allows the production of non N₂-diluted syngas, solves the aforementioned problem of high concentrations of tars and CO₂ emissions, while avoiding the need of ASU. In CLG, fuel gasification and heat generation are divided into two stages carried out in two interconnected fluidized bed reactors. An oxygen carrier is used instead of an inert solid to transport heat and oxygen between

reactors. In addition, this material is also capable of catalyzing tar reforming reactions, reducing the tar concentration and therefore minimizing the corrosion of the reactors and the blockage of the pipes as well as other problems caused in downstream processes.

Although fossil fuels, such as coal or petroleum coke, can be used for the gasification process, one of the additional advantages of this technology is the production of renewable syngas when biomass is used as fuel. Biomass, an abundant natural resource derived from plants and organic waste, is considered carbon neutral since it absorbs the same amount of carbon from the atmosphere during its growth as it releases when is consumed as fuel. Thus, when the use of biomass is combined with CO₂ capture technologies, negative CO₂ emissions can be achieved, which is one of the goals to achieve net zero emissions by 2050 [2].

The main scheme of the CLG process is shown in Fig. 1. The fuel is fed into the fuel reactor (FR) where it is devolatilized, generating mainly a gaseous fraction (CO, CO₂, H₂, CH₄ and H₂O) and a solid fraction (char). The solid fraction is gasified with steam, which is also used for fluidization and is fed from the bottom of the FR. Both the volatile products and the gases coming from char gasification react with the oxygen carrier, reducing it. Once reduced, the oxygen carrier passes to the air reactor (AR) where it is regenerated with air, heating up due to the exothermic nature of the oxidation reaction. Finally, the oxidized

* Corresponding author.

E-mail address: ldediego@icb.csic.es (L.F. de Diego).

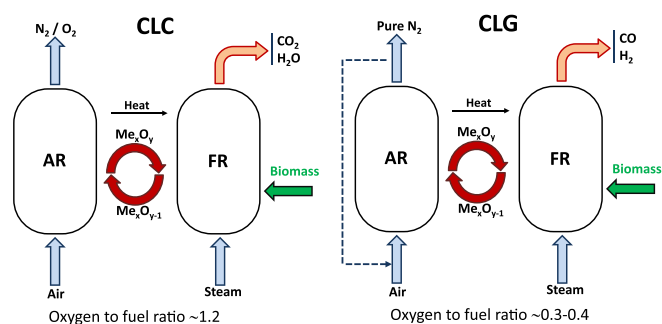


Fig. 1. Scheme of the CLC and CLG processes.

oxygen carrier enters into the FR again transferring the heat necessary for devolatilization and gasification reactions.

Unlike chemical looping combustion (CLC), where oxygen is fed (oxygen-fuel ratio ~ 1.2) and transported in excess to ensure full combustion of the fuel, in CLG, the oxygen transferred from the AR to the FR must be controlled to avoid full oxidation of the volatiles and gasification products. In this sense, low oxygen-fuel ratios ($\sim 0.3\text{--}0.4$) are used, leading the process to high reducing atmospheres. For this reason, several authors have focused their research on the development of resistant oxygen carriers to these highly reducing conditions existing in the CLG process.

Natural ores have been tested in continuous units due to their low cost and abundance. One of the most studied oxygen carriers is hematite, a natural iron ore. This Fe-ore, diluted with silica sand, was used in a 25 kW_{th} unit for gasification of rice husk [3] and coal [4], and some agglomeration was found at high temperatures (900 °C). Hematite has also been tested by our research group on a 1.5 kW_{th} unit installed at Instituto de Carboquímica (ICB-CSIC), giving lifetimes of 300 h [5]. This lifetime was much lower than the more than 2000 h obtained using the same oxygen carrier in CLC [6]. Other minerals, such as ilmenite, have also been investigated by our research group, showing good behavior but reducing their lifetime to almost half of that obtained in combustion [7]. LD slag, a by-product from the steel production, was tested in the same unit and a low lifetime (300 h) was also found [8].

In spite of their higher costs, synthetic oxygen carriers have been prepared to improve the lifetime relative to ores and wastes. According to the principles of reactivity, abundance and environmental harmlessness, Fe-based synthetic oxygen carriers have been widely developed for CLG. There are some works that study the use of pure Fe₂O₃ [9], but its low resistance makes it practically unfeasible for CLG. The addition of Fe₂O₃ to an inert support (commonly Al₂O₃) was raised as a promising way to reduce costs and increase the lifetime of the particles due to the high strength of the support. High resistance to redox cycles without sintering was observed in a 10 kW_{th} continuous unit operating with an oxygen carrier composed of 70 wt% Fe₂O₃ and 30 wt% alumina and prepared by a mechanical mixing method [10]. This oxygen carrier also showed relatively high resistance to attrition after 60 h of operation [11].

Our research group at ICB-CSIC developed a 20 wt% Fe₂O₃ over alumina oxygen carrier (Fe20Al) prepared by the hot wetness impregnation method [12]. The Fe20Al oxygen carrier was satisfactorily tested for the combustion of sour and acid gas combustion [13,14] as well as for the combustion of liquid fuels [15]. Furthermore, the Fe20Al oxygen carrier proved to be a promising solid for CLC of CH₄, as it retained its properties after numerous redox cycles, with a lifetime of 1100 h [16]. Due to the great results obtained in CLC, the analysis of the behavior of this oxygen carrier for CLG was also carried out in a continuous unit [17]. It was found that, similar to what happened with ores and waste, the lifetime of the oxygen carrier decreased from 1100 h working in CLC conditions to 350 h working in CLG conditions. Structural analysis of used oxygen carrier particles revealed that the migration of Fe had

affected them, creating an outer layer that detached after repeated cycles, compromising the integrity of the particles and reducing their oxygen transport capacity. Some authors [18,19] explained that Fe cations are displaced to the surface of the particles after cyclic redox reactions, generating a porous structure inward. It was suggested that the Fe outer layer hindered the diffusion of gases into the interior of the particle. Ma et al. [20] found that increasing the calcination temperature of FeAl oxygen carriers led to a reduction in pore volume and a more compact particle microstructure, which promoted the outward migration of Fe cations in the oxygen carrier. To prevent Fe segregation and the formation of a Fe layer, the authors suggested that particle calcination at lower temperatures (900 °C–1100 °C) should be used in order to maintain porosity and allow gas diffusion inward. Another study found that decreasing the Fe₂O₃ concentration in the oxygen carrier particles from 25 wt% to 10 wt% improved the lifetime of the particles from 100 h to 900 h [21]. Analysis of particles used in a pilot plant for about 50 h showed that the oxygen carrier particles with a Fe₂O₃ content of 10 wt% had hardly any losses of Fe₂O₃, while particles with 20 wt% and 25 wt% of Fe₂O₃ had lost 13 % and 23 % of the initial Fe₂O₃ content, respectively.

As has been commented so far, Fe₂O₃/Al₂O₃ oxygen carriers have a notable relevance in chemical looping technologies, but their behavior is very sensitive to the atmosphere in which they operate and to the properties generated during their preparation, being the lifetime and the reactivity conditioned by these parameters. Although lifetimes values and microstructure analysis of the oxygen carriers have been determined in previous works, most of these studies have been focused on the analysis of the effect of operating parameters, such as reactor temperature and oxygen-fuel ratio, on the behavior of the process, mainly in the yields achieved and the composition of the syngas generated in the process. Therefore, to the best of our knowledge, the isolated effect of operating conditions on the solid structure of oxygen carrier particles has not been studied in detail.

The aim of the present study was to analyze the isolated effect of preparation and operating conditions on the solid structure of oxygen carrier particles, as this can provide insights into the fundamental mechanisms that govern the behavior of the oxygen carrier in Chemical Looping systems. By understanding the structural changes that occur in the oxygen carrier particles under different operating conditions, it may be possible to optimize the preparation and operation of oxygen carriers to achieve higher reactivity and longer lifetimes. Furthermore, understanding the effect of operating conditions on the solid structure of oxygen carrier particles can help in the development of more robust and efficient Chemical Looping technologies. This knowledge can be used to improve the design and operation of Chemical Looping systems, with the goal of reducing the environmental impact of syngas or energy production and increasing the sustainability of syngas or energy generation.

2. Experimental

2.1. Oxygen carriers

Three samples of synthetic Fe-based oxygen carriers were prepared by the hot wetness incipient impregnation method. γ -alumina (Puralox NWA-155, Sasol Germany GmbH) of 0.1–0.3 mm, with a density of 1.3 g/cm³ and a porosity of 55.4 %, was used as the support. The alumina was preheated at 80 °C in a planetary mixer and successive impregnations (see Table 1) of a hot solution of iron nitrate (3.8 M) from Panreac were added depending on the final iron concentration required. Calcination at 550 °C for 30 min after each impregnation was performed to decompose iron nitrate into Fe₂O₃. A final sintering of 2 h in air atmosphere at 950 °C was carried out to increase the strength of the particles. The materials prepared were Fe10Al (10 wt% of Fe₂O₃), Fe20Al (20 wt% Fe₂O₃), and Fe25Al (25 wt% Fe₂O₃). Table 1 shows the main physical and chemical properties of the prepared oxygen carriers.

Microstructural images of fresh and used oxygen carrier particles

Table 1
Physical and chemical properties of fresh oxygen carriers.

		Fe10Al	Fe20Al	Fe25Al
Fe ₂ O ₃ content*	wt.%	10 ± 0.1	20 ± 0.2	25 ± 0.2
Number of impregnations		1	2	3
Oxygen transport capacity, R _{oc} **		0.010	0.020	0.025
Particle size	µm	100–300	100–300	100–300
Skeletal density	kg/m ³	3744 ± 55	3950 ± 60	4105 ± 61
Crushing strength	N	1.8 ± 0.5	1.5 ± 0.4	1.6 ± 0.5
Porosity	%	50.2 ± 0.4	45.6 ± 0.4	44.4 ± 0.4
XRD phases		Fe ₂ O ₃ , α-Al ₂ O ₃ , θ-Al ₂ O ₃		

* Fe metal content determined by ICP-OES.

** Determined in a thermogravimetric analyzer.

were taken by a Hitachi S-3400 N scanning electron microscope (SEM) coupled to a Roentec XFlash Si (Li) detector for energy-dispersive X-ray (EDX) analysis. Crystalline phases present in each carrier were determined using a Bruker D8 Advance A25 polycrystalline powder X-ray diffractometer (XRD). Inductively Coupled Plasma - Optical Emission Spectroscopy (ICP-OES) was used to determine Fe-content in the oxygen carriers by a Xpctroblue-EOP-TI FMT26 (Spectro) spectrophotometer.

2.2. Experimental procedure

Long-term tests were conducted in a CI Electronics thermogravimetric analyzer (TGA) described elsewhere [22]. The tests were performed using samples of ~150 mg of fresh oxygen carrier, which were exposed to alternate reducing and oxidizing atmospheres during 300 redox cycles. A mixture of 15 vol% CO and 25 vol% CO₂ was used as the reducing agent and 3 vol% O₂ as the oxidizing agent (N₂ balance). The total gas flow in all cases was 25 Nl/h. Between each reduction and oxidation period, a purge period with N₂ was introduced for 2 min to avoid gas mixing.

The sample conversion variation (ΔX_s) during the reduction and oxidation periods was limited by controlling the reaction time and was defined by Eqs. (1)–(3).

$$\Delta X_s = X_{oxi} - X_{red} \quad (1)$$

$$X_{oxi} = 1 - \frac{m_{oxi} - m}{m_{oxi} - m_{red}} \quad (2)$$

$$X_{red} = \frac{m_{oxi} - m}{m_{oxi} - m_{red}} \quad (3)$$

where m was the actual mass of sample, m_{oxi} was the mass of the sample fully oxidized (Fe₂O₃·Al₂O₃) and m_{red} the mass of the sample in the reduced form (FeAl₂O₄). The redox pair for Fe-Al solids was Fe₂O₃·Al₂O₃-FeAl₂O₄, since FeAl₂O₄ was the only reduced state permitted by thermodynamics, as reported by Cabello et al. [23]. Further reduction to

metallic Fe was not possible in the presence of steam or CO₂, which is common both in CLC and CLG.

Three ranges of ΔX_s were analyzed, which are schematically shown in Fig. 2. a) $\Delta X_s = 25\%$ starting with the sample fully reduced, that is, from $X_{oxi} = 0\%$ ($X_{red} = 100\%$) to $X_{oxi} = 25\%$, b) $\Delta X_s = 25\%$ finishing with the sample fully oxidized, that is, from $X_{oxi} = 75\%$ to $X_{oxi} = 100\%$, and c) $\Delta X_s = 100\%$, complete cycles from $X_{oxi} = 0\%$ to $X_{oxi} = 100\%$. The ΔX_s in the CLG process depends mainly on the solids circulation rate and Fe₂O₃ content in the oxygen carrier. For the Fe₂O₃ contents used in this work (10 wt% to 25 wt%) and using typical solids circulation rates (5–7 kg/MW.s) to avoid a large variation between temperatures in FR and AR ($\Delta T = 50$ – 80 °C), ΔX_s would be between 10 and 40 %, as stated by a previous work [24]. So, a $\Delta X_s = 25\%$ was considered a realistic value to use with all three oxygen carriers. Moreover, taking into account that in the FR the oxygen carrier is almost completely reduced, the conversion variation in the process must be between 0 and 25 %. On the contrary, in the CLC process, excess oxygen is used and the oxygen carrier leaves the AR almost completely oxidized ($X_{oxi} = 100\%$). A conversion variation of $\Delta X_s = 25\%$ (75–100 %) corresponds to a ϕ (amount of the oxygen available in the FR reactor, which is transported by the oxygen carrier, with respect the stoichiometric oxygen demanded by the fuel fed) value of 4, which is a very typical value for the CLC process. The $\Delta X_s = 100\%$ has been used for comparative purposes.

After the completion of the cycles in TGA, the reactor was cooled under N₂ atmosphere before the sample extraction. Then, the microstructure of some selected particles after reaction was analyzed by SEM-EDX.

3. Results

In this study, the evolution of the microstructure of oxygen carrier particles during redox cycles was analyzed in relation to oxygen carrier conversion, temperature, Fe₂O₃ content, and number of redox cycles. A total of twenty-seven experiments were conducted in TGA, each consisting of 300 redox cycles, covering a range from the most aggressive conditions for the oxygen carrier (high temperature and high reducing atmosphere) to the mildest conditions (low temperature and low reducing atmosphere), which represent typical CLG and CLC conditions.

Fig. 3 illustrates an example of redox cycles performed with the Fe20Al oxygen carrier at a temperature of 950 °C and a sample conversion range from $X_{oxi} = 0\%$ to $X_{oxi} = 100\%$. Under these conditions, significant degradation or weakening of the oxygen carrier particles was observed. However, as can be seen in the figure, despite the decrease in the mechanical resistance of the solid, the mass variation remained constant during all cycles, indicating that the oxygen transport capacity of the oxygen carrier did not vary. Moreover, it was found that the reactivity of the particles remained constant during the 300 cycles, with both the reduction and the oxidation being quickly at the beginning and end of the test. The same effect was observed in all experiments, with the

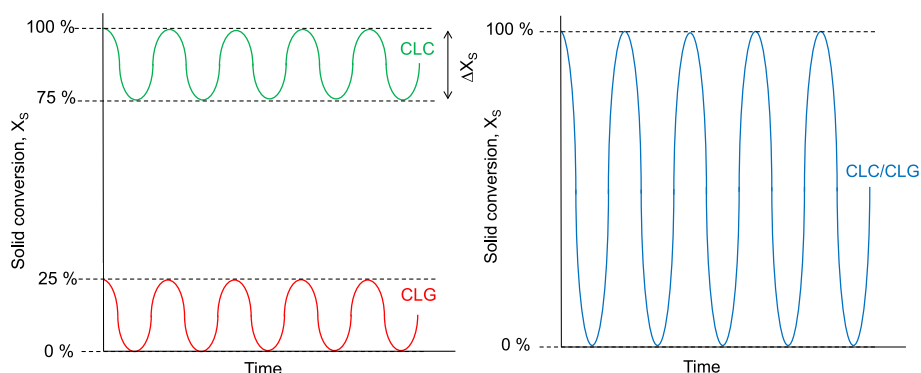


Fig. 2. Oxygen carrier conversion. (a) $\Delta X_s = 25\%$, (b) $\Delta X_s = 100\%$.

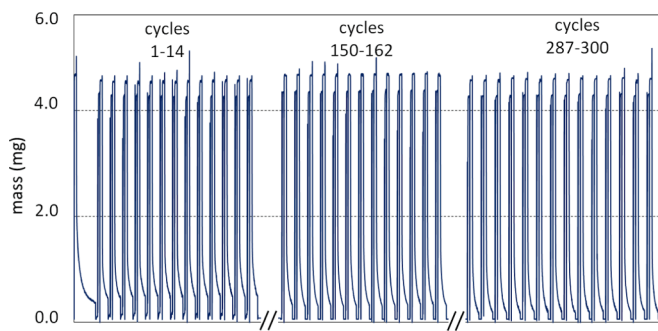


Fig. 3. Redox cycles performed with the Fe₂O₃ oxygen carrier in the TGA. $\Delta X_s = 100\%$, $T = 950\text{ }^\circ\text{C}$.

different oxygen carriers and under the different experimental conditions, whether or not degradation or weakening of the particles occurred.

3.1. Evaluation of isolated parameters

3.1.1. Effect of oxygen carrier conversion

When the CLC process is performed, excess lattice oxygen is transported from AR to FR to achieve complete combustion of the fuel. In this case, the oxygen carrier should be fully oxidized in the AR, while its reduction in the FR will depend mainly on its oxygen transport capacity and solid circulation rate for a given fuel supply. Consequently, the variation in solid conversion (ΔX_s), as defined by Eqs. (1)–(3), will be limited to a range of $X_{\text{oxi}} = 100\%$ ($X_{\text{red}} = 0\%$) in the AR and X_{oxi} greater than 0% and $X_{\text{red}} < 100\%$ in the FR (see Fig. 2).

Unlike the CLC process, the CLG process is conducted under sub-stoichiometric conditions to prevent complete combustion of the fuel. This implies that the amount of oxygen transported from AR to FR must be carefully controlled to ensure that there is sufficient oxygen transfer to meet the energy balances and achieve autothermal operation. In other words, it is necessary to adjust the oxygen to fuel ratio to maximize syngas yield while operating under autothermal conditions. Various

methods have been used in the literature to control this oxygen to fuel ratio [24]. One of them is based on the variation of the biomass fed for a constant transfer of lattice oxygen [4]. However, this method causes variations in the solids specific inventory in the fuel reactor. Dilution of the oxygen carrier with an inert material has been done in another method, but different attrition rates of the solids could vary the solid mixture with time [3]. Another possibility would be to limit the oxygen transferred by controlling the solids circulation flow rate between reactors, but it could affect to fluidynamic behavior [24]. Finally, recent studies have reported that the limitation of oxygen supply in AR allows maintaining a stable solids circulation rate while maintaining a constant solid inventory and the fluidynamic conditions [24,25], it means without disturbing reactor hydrodynamics. This control method concept has been demonstrated to be suitable for small prototypes [5,7,8,17,21] and large-scale (1 MW_{th}) CLG units [26,27]. In this control method, oxygen limitation causes incomplete oxidation of the oxygen carrier in AR, $X_{\text{oxi}} < 100\%$, while in FR the solid can be reduced to the lowest state allowed by thermodynamics ($X_{\text{oxi}} = 0\%$, $X_{\text{red}} = 100\%$), which is FeAl₂O₄. In any case, the variation of the oxygen carrier conversion will depend on the operating conditions employed in the process and this parameter will affect the structure of the particles, being identified as the main reason for the decrease in the oxygen carrier lifetime when it is used under CLG conditions as opposed to CLC conditions [28]. In this section, the behavior of the oxygen carriers during redox cycles at different atmospheres and three different degrees of conversion (X_{oxi} from 75 % to 100 %, from 0 % to 25 %, and from 0 % to 100 %) was analyzed.

Fig. 4 shows SEM images of the microstructure of the Fe₂O₃ oxygen carrier particles taken after 300 redox cycles at a temperature of 950 °C and three different degrees of conversion. The SEM images revealed that operating with low variations of oxygen carrier conversion in reducing atmospheres ($\Delta X_s = 0\text{--}25\%$), corresponding to typical operating conditions in CLG, promoted the migration of internal Fe to the surface of the particles (see Figure S3 in the Supplementary Material). The same phenomenon was observed when redox cycles were carried out with high oxygen carrier conversion variations, from full reduction to full oxidation ($\Delta X_s = 0\text{--}100\%$). In both samples, a rough and highly porous

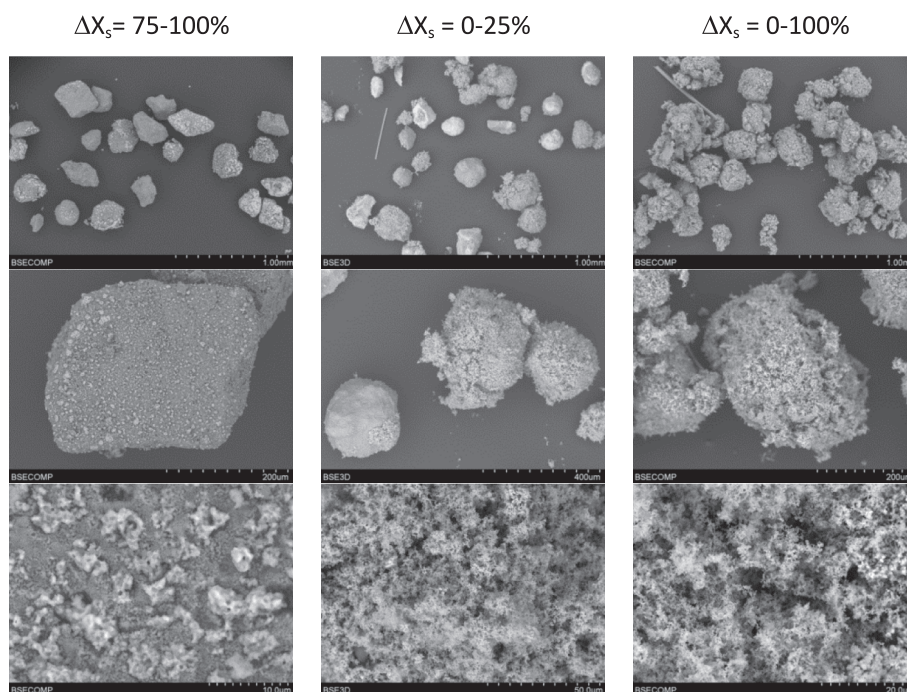


Fig. 4. SEM images of the Fe₂O₃ particles after 300 redox cycles in TGA. $T = 950\text{ }^\circ\text{C}$. Three different ranges of conversion: $\Delta X_s = 75\text{--}100\%$, $\Delta X_s = 0\text{--}25\%$, and $\Delta X_s = 0\text{--}100\%$.

layer with a filamentous shape and ramifications was observed on the surface of the particles. The SEM images also revealed the presence of agglomerates, which linked the oxygen carrier particles forming new large particles. Beyond the formation of agglomerates, Fe migration resulted in an increase in the volume of the particles, as shown in [Figure S1, Series a, in Supplementary Material](#). In addition, the migration of Fe led to a decrease in the mechanical strength of the solid, making them more susceptible to the attrition process. In contrast, the sample taken from the experiment conducted under more typical conditions of the CLC process ($\Delta X_s = 75\text{--}100\%$) showed a surface with negligible iron deposition. Only a few small iron grains were found on the surface of the particles, likely formed during the impregnation preparation process. The particles showed similar sizes with irregular shapes and no signs of agglomeration. Compared to the samples obtained under more reducing conditions, the surface of these particles was compact, less porous, and had fewer rough structures. Thus, it can be concluded that the migration of Fe, and consequently the degradation of the Fe-based oxygen carrier particles, was significantly reduced under oxidizing conditions. These findings are consistent with previous results obtained from a continuously operating unit, which determined a decrease in the lifetime of the Fe20Al oxygen carrier particles from 1100 h in CLC to 300 h in CLG [\[21\]](#).

3.1.2. Effect of temperature

Typical operating temperatures at CLG ranged from 750 to 940 °C [\[3,4,10,11\]](#). However, previous CLG studies have reported that operating at FR temperatures above 900 °C can bring several benefits for the gasification process, including an increase in the char gasification rate, a reduction in tars, and higher conversion of hydrocarbons into CO and H₂ [\[17,21\]](#). On the contrary, high temperature can also have negative impact on the integrity of the oxygen carrier particles. In this study,

Fe20Al oxygen carrier samples were used to analyze the microstructure of the particles after undergoing 300 redox cycles in the conversion range from $\Delta X_s = 0\%$ to 25% at three different temperatures (850 °C, 900 °C and 950 °C) to cover a wide range of temperatures commonly used in BCLG.

[Fig. 5](#) shows SEM images of the oxygen carrier particles after 300 redox cycles. It can be observed that the particles reacted at 850 °C retained their integrity and showed similar sizes with irregular shapes. Their surface was compact, with low porosity and rugosity, and without signs of agglomeration. A few small iron grains were visible on the particle surface, likely formed during the impregnation preparation process, as previously mentioned. Thus, it can be inferred that low migration of Fe occurred under this operating condition. As the temperature increased first to 900 °C and then to 950 °C, a progressive growth of iron grains was observed on the surface of the particles. This was a consequence of the increased migration of Fe cations from the inward to the external surface of the oxygen carrier. As discussed in the previous section, iron migration promoted Fe accumulation around the particles, creating a highly iron-concentrated outer layer with a rough and spongy structure (see [Figure S3 in the Supplementary Material](#)). At both 900 °C and at 950 °C, the appearance of iron agglomerates on the particle surface and the formation of small particles composed mainly of iron due to particle disintegration were observed. Again, the migration of Fe increased the porosity of the particles, with greater porosity at higher temperatures, resulting in a notable increase in particle volume (see [Figure S1, Series b, in Supplementary Material](#)). This also promoted a decrease in particle mechanical strength, which could cause the particles to break easily during actual operation in a fluidized bed reactor. In this regard, it is recommended to operate at low temperatures to preserve the integrity of the oxygen carrier particles.

The effect of temperature was also analyzed using the Fe10Al and

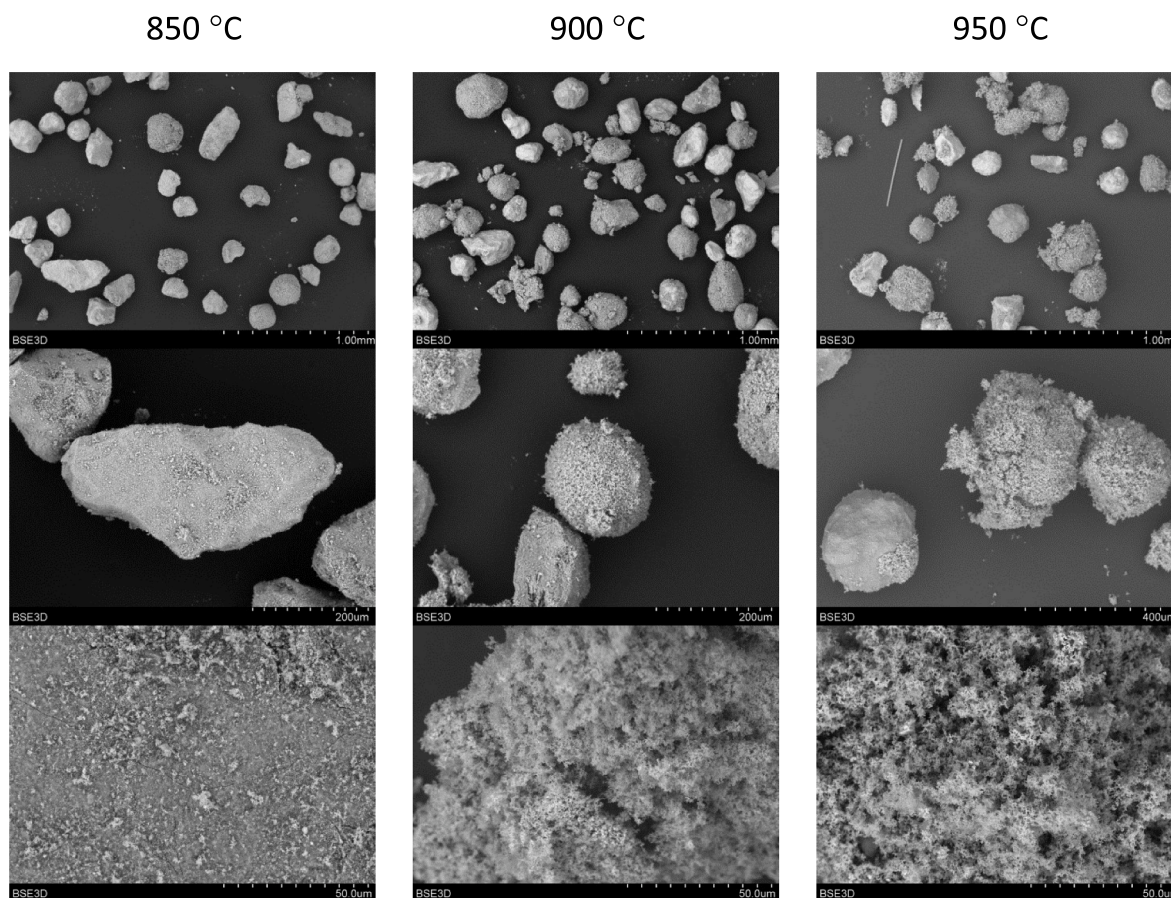


Fig. 5. SEM images of the Fe20Al particles after 300 redox cycles at 850 °C, 900 °C and 950 °C. $\Delta X_s = 0\text{--}25\%$.

Fe25Al oxygen carriers. Similar to Fe20Al, it was observed that iron migration increased with an increase in temperature for both oxygen carriers. However, it was also found that high particle weakening occurred in the Fe25Al oxygen carrier even at the lower temperature of 850 °C. This suggests that the Fe₂O₃ content in the oxygen carrier also had an influence on particle integrity.

3.1.3. Effect of Fe₂O₃ content

In CLG, the use of oxygen carriers with a wide range of oxygen transport capacities is advantageous over CLC, as the amount of oxygen transported from the AR to the FR needs to be controlled to prevent complete combustion of the fuel. This allows for varying the Fe₂O₃ content in the oxygen carrier to improve its mechanical properties. In this study, the microstructure of reacted particles of three FeAl oxygen carriers with Fe₂O₃ contents of 10 wt%, 20 wt%, and 25 wt% was analyzed.

Fig. 6 shows SEM images of the particles of the three oxygen carriers tested in TGA for 300 redox cycles at the temperature of 900 °C and a ΔX_s from 0 % to 25 %. The SEM images show that the Fe20Al and Fe25Al oxygen carriers experienced high iron migration, resulting in the appearance of iron agglomerates on the surface of some of the particles and forming new particles with different shapes and sizes. In contrast, the Fe10Al oxygen carrier exhibited a much more stable structure, with a slightly higher Fe concentration observed on the outer particle. The grain sizes of Fe located in the outer layer of the Fe10Al particles were very small compared to those formed on the Fe20Al and Fe25Al. Moreover, the external surface of the Fe20Al and Fe25Al particles also showed a more porous, spongy, and rough structure than the Fe10Al particles. This suggests that low interactions between metal oxide and the support preserved the oxygen carrier structure. Cabello et al. [28] suggested that the low interaction between the metal and the support

promotes low volumetric changes, avoiding the generation of vacancies that are responsible for the weakening of the particles.

These results show that the stability of Fe-based oxygen carriers in chemical looping processes is affected by the initial Fe₂O₃ content in the oxygen carrier, and those oxygen carriers with lower Fe₂O₃ content tend to be more stable. The implication of this finding is important in the preparation of oxygen carriers, since the use of oxygen carriers with a low amount of active phase reduces their preparation costs. The optimal amount of active phase in the oxygen carrier will depend on the specific requirements of the process it will be used in. A higher amount of active phase (i.e. higher Fe₂O₃ content) will be necessary for the CLC process, where complete combustion of the fuel is desired, compared to the CLG process, where oxygen transport must be controlled to prevent complete combustion of the fuel. Therefore, for the CLG process, an oxygen carrier with a lower amount of active phase, such as the Fe10Al oxygen carrier, would be sufficient to transport the necessary oxygen [24]. However, for the CLC process, an oxygen carrier with a higher Fe₂O₃ content would be necessary.

3.1.4. Effect of number of cycles

In the previous sections, it was shown that the degradation and loss of mechanical strength of Fe-based oxygen carriers are strongly related to the operating parameters and the intrinsic characteristics of the oxygen carrier. The degradation of the particles does not occur immediately, but is a consequence of the thermal and chemical stress experienced by the particles due to redox cycles. Therefore, in order to analyze the evolution of the behavior of oxygen carriers, this section analyzes the evolution of the structure of the particles as a function of the number of redox cycles they undergo. To accomplish this, samples of Fe20Al and Fe25Al oxygen carriers were subjected to 25, 50, 100, and 300 cycles and subsequently analyzed using SEM. The TGA experiments

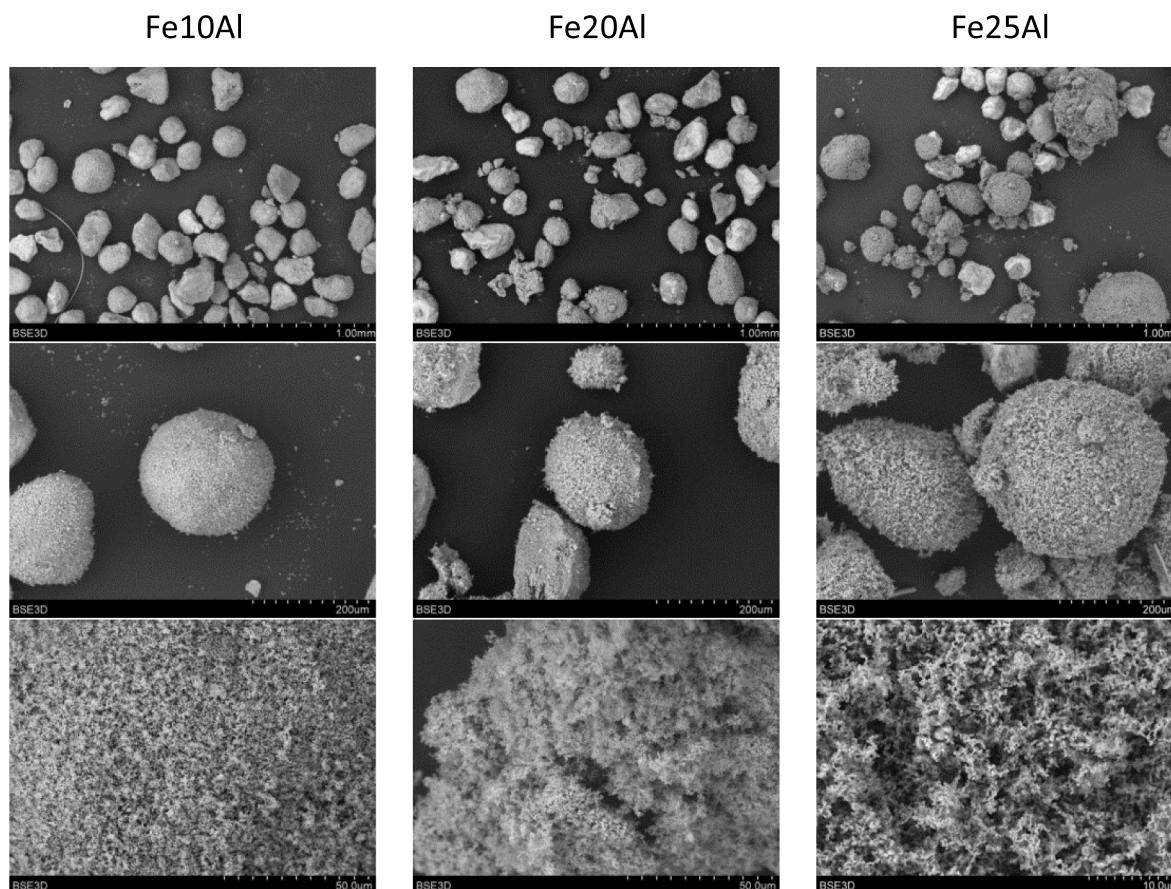


Fig. 6. SEM images of the Fe10Al, Fe20Al and Fe25Al particles after 300 redox cycles at 900 °C. $\Delta X_s = 0-25$ %.

were conducted under highly reducing conditions ($\Delta X_s = 0\text{--}25\%$) at the temperature of $900\text{ }^\circ\text{C}$. It should be noted that a new fresh sample was used for each set of redox cycles.

Fig. 7 and Fig. 8 show SEM images of oxygen carrier particles taken after each set of redox cycles. It can be observed that the migration of Fe and the degradation of the particles were progressive with the number of redox cycles. Fresh particles and those used for only a few redox cycles (50 with Fe20Al and 25 with Fe25Al) showed a compact surface, with low porosity and roughness, and no large Fe grains or agglomerates were observed on the surface. As the number of redox cycles increased, the migration of Fe became evident, and small grains or agglomerates of Fe formed on the surface of the particles (images after 100 cycles for the Fe20Al oxygen carrier and 50 for the Fe25Al oxygen carrier). The size of the Fe grains or agglomerates grew with the number of cycles, forming an external layer concentrated in Fe, which showed high porosity and roughness (See Figure S2 in the Supplementary Material). After 300 redox cycles, it was observed that some particles had broken into pieces, while others had joined together due to agglomeration, generating larger particles.

Finally, it should be noted that the process of Fe migration and particle degradation was faster in the Fe25Al oxygen carrier than in the Fe20Al carrier due to its higher initial Fe_2O_3 content, which is in complete agreement with what was observed in the previous section.

4. Discussion and practical information

Previous studies have demonstrated the potential of Fe-based oxygen carriers supported on Al_2O_3 ($\text{Fe}_2\text{O}_3/\text{Al}_2\text{O}_3$) for application in both CLC and CLG processes [12–17,21]. However, most of these studies have focused on analyzing the effects of varying operating conditions, such as temperature, oxygen/fuel ratio, steam/fuel ratio, etc. While important for evaluating process parameters such as combustion efficiency, CO_2 capture, syngas composition and yield, and tar formation, this approach makes it difficult to accurately analyze the effect of each individual operating condition on the physicochemical evolution of the oxygen carrier particles, as the particles are exposed to very different operating conditions throughout the experimental campaign. Nonetheless, the results obtained in this study will be compared to those obtained in a $1.5\text{ kW}_{\text{th}}$ prototype with continuous operation using the same oxygen carriers under CLG conditions, while keeping these considerations in mind

[17,21]. The prototype consisted of two bubbling fluidized bed reactors, air reactor (0.08 m id) and fuel reactor (0.05 m id), interconnected through a loop seal (0.03 m id) which prevented gas mixing between reactors. Pine sawdust, from the locality of Ansó (Spain), was used as fuel. Further description of this unit could be found elsewhere [29].

Table 2 presents a summary of the results obtained in this study regarding the integrity of the particles of the three oxygen carriers after being subjected to 300 redox cycles in a TGA under different operating conditions. From these results, the following important conclusions can be drawn:

- The conversion variation and the degree of reduction/oxidation of the oxygen carrier particles during redox cycles are parameters that strongly affect the evolution of their mechanical stability. In samples with high degrees of oxidation, typical for CLC operating conditions, the mechanical stability of the particles is preserved longer as the solids conversion variation decreases. It can be seen in Table 2 that the mechanical stability of the solids in the range $\Delta X_s = 75\text{--}100\%$ was higher than in the range $\Delta X_s = 0\text{--}100\%$. On the contrary, in samples with high degrees of reduction, typical for CLG operating conditions, the mechanical stability of the particles is preserved for a longer time as the solids conversion variation increases. The mechanical stability of the solids in the range of $\Delta X_s = 100\%$ was higher than in the range of $\Delta X_s = 0\text{--}25\%$. Therefore, it is preferred to operate at ΔX_s close to 100% instead of a low ΔX_s range. This could be achieved by using oxygen carriers with low Fe_2O_3 content because the lower the oxygen transport capacity, the higher the solid conversion variation during the redox cycles.
- The Fe_2O_3 content in the oxygen carrier has little effect on preserving the mechanical stability of the particles when working under CLC conditions (oxidizing atmosphere), but it is a decisive characteristic in the selection of the oxygen carrier when working under CLG conditions (reducing atmosphere). For CLG, it is advisable to use as little Fe_2O_3 as possible in the preparation of the oxygen carrier. This would also help to achieve high solid conversion variations, which have been found to be beneficial in maintaining particle mechanical stability. However, it must be noted that the oxygen carrier must have sufficient oxygen transport capacity, R_{OC} , to transfer the oxygen needed to maintain the system in autothermal operation.

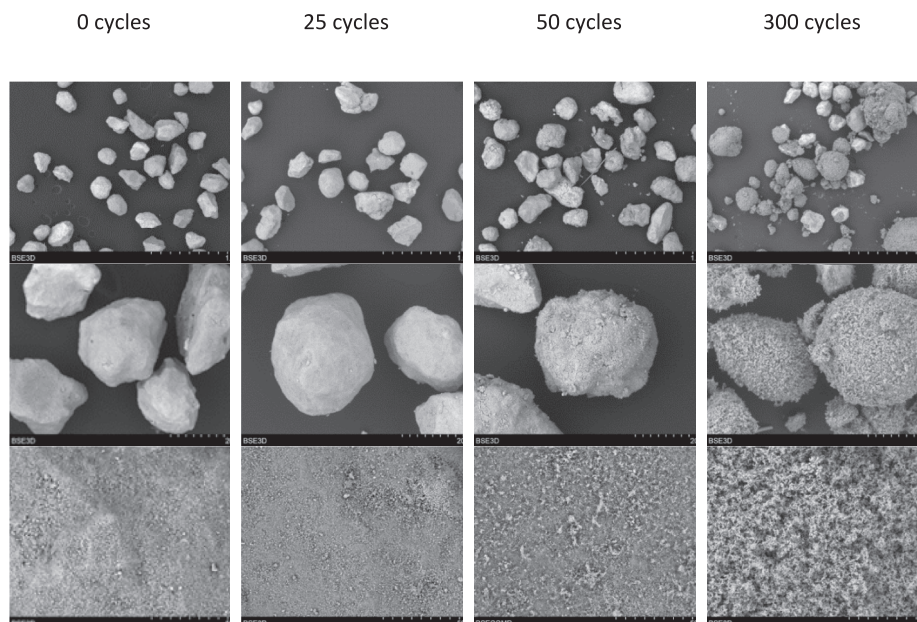


Fig. 7. SEM images of the Fe25Al oxygen carrier particles after a set number of redox cycles. $T = 900\text{ }^\circ\text{C}$. $\Delta X_s = 0\text{--}25\%$.

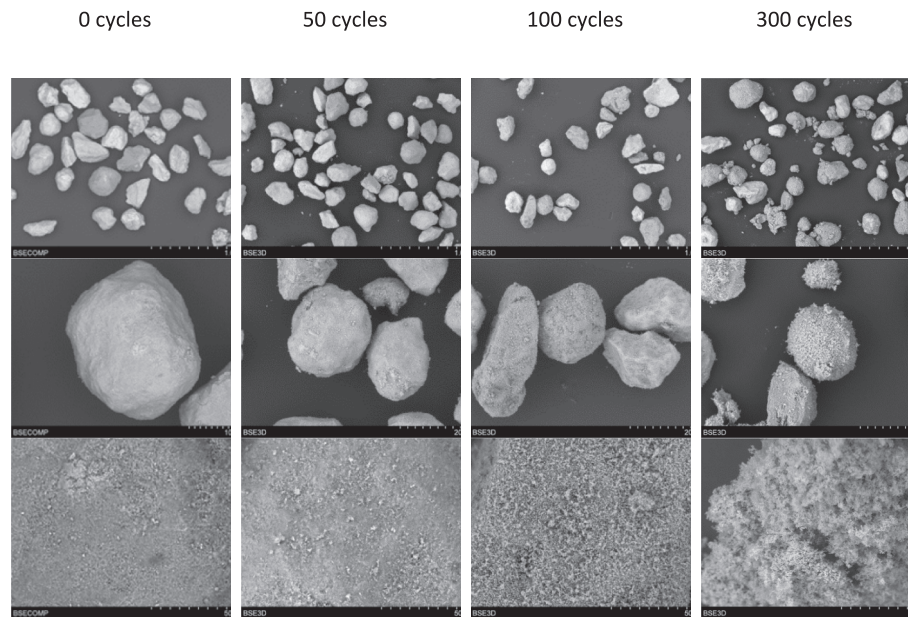


Fig. 8. SEM images of Fe20Al oxygen carrier particles after a set number of redox cycles. $T = 900\text{ }^{\circ}\text{C}$. $\Delta X_s = 0\text{--}25\%$.

Table 2

Integrity of the oxygen carrier particles after 300 redox cycles in TGA and oxygen carrier particle lifetime determined in a $1.5\text{ kW}_{\text{th}}$ prototype operating under CLG conditions. (P = Preserved integrity, L = loss of integrity).

		←CLG→				
		←CLC→				
		$\Delta X_{\text{oxi}} (\%)$			1.5 kW _{th} CLG unit	
Solid	T (°C)	0-25	0-100	75-100	Lifetime (h)	Ref
Fe10Al	850	P	P	P	900	[21]
	900	p	P	P		
	950	L	P	P		
Fe20Al	850	P	P	P	350	[17]
	900	L	P	P		
	950	L	L	P		
Fe25Al	850	L	P	P	100	[21]
	900	L	L	P		
	950	L	L	P		

Less reducing atmosphere →

- An increase in the operating temperature results in a higher rate of degradation of the oxygen carrier particles. This negative influence is particularly important in very reducing operating conditions, typical of the CLG process, and is aggravated when working with low degrees of solids conversion variation.

Table 2 also shows the oxygen carrier lifetimes determined based on measured attrition rates in a $1.5\text{ kW}_{\text{th}}$ prototype. For CLG operating conditions, the oxygen carrier lifetime decreased as the Fe_2O_3 content in the particles increased. Lifetimes of 900, 350, and 100 h were found for the oxygen carriers with 10 wt%, 20 wt%, and 25 wt% of iron oxide, respectively. Therefore, it is concluded that the evolution of the mechanical stability of the solid particles determined in the tests carried out in a TGA is directly related to the lifetime inferred through the attrition rate measured in the operation of a CLG prototype. Thus, the Fe25Al oxygen carrier, which had a lifetime of 100 h in a $1.5\text{ kW}_{\text{th}}$ CLG continuous unit, only preserved its mechanical stability when

performing redox cycles in the TGA in the solid conversion range $\Delta X_s = 75\text{--}100\%$ or performing complete conversion cycles but at low temperature ($850\text{ }^{\circ}\text{C}$). In contrast, the Fe10Al oxygen carrier preserved its mechanical stability in most experiments carried out in TGA, except the one conducted at $950\text{ }^{\circ}\text{C}$ with a solid conversion variation from $\Delta X_s = 0\text{--}25\%$. This result is related to the 900 h lifetime obtained in the continuous unit, which corresponded to the longest lifetime found among the three oxygen carriers. Therefore, the method used in this work was perfectly capable of anticipating the oxygen carrier lifetime in continuous units by performing redox cycles in TGA.

There is no information available on the effect of operating temperature on the mechanical stability of oxygen carrier particles in prototypes. However, previous tests on CLG prototypes have shown that increasing the temperature improved gasification parameters such as fuel conversion, carbon conversion efficiency, cold gas efficiency, and tar reduction. Therefore, taking into account that in this work it has been found that an increase in the temperature of operation resulted in a

higher rate of degradation of the oxygen carrier particles, the optimal working temperature will be a compromise between the costs of renewing the solid at the end of its useful life and the improvement of the parameters of the CLG process.

5. Conclusions

Long-term tests, consisting of 300 redox cycles, were carried in a TGA to study the effect of solid conversion variation and oxidation state after redox cycles, Fe_2O_3 content, and reacting temperature on the behavior of Fe-based oxygen carrier particles ($\text{Fe}_2\text{O}_3/\text{Al}_2\text{O}_3$). The microstructure of the oxygen carrier particles generated in these tests was analyzed by SEM to obtain information on the effect of the operating conditions on the mechanical stability of the samples. The following conclusions were drawn:

- The solid conversion variation and degree of reduction/oxidation during redox cycles strongly influenced the evolution of the mechanical stability of the oxygen carrier particles. The mechanical integrity of the particles was preserved for a longer time as the solids conversion variation decreased under typical CLC operating conditions, and as the solids conversion variation increased under typical CLG operating conditions.
- The Fe_2O_3 content in the oxygen carrier had a significant impact on the preservation of the mechanical integrity of the particles when operating under CLG conditions. The lower the Fe_2O_3 content in the particles, the greater their stability in redox cycles.
- An increase in the reaction temperature led to a more rapid degradation of the oxygen carrier particles. This negative influence was aggravated when operating under very reducing operating conditions and with low solids conversion variations.
- The oxygen carrier characterization method used in this study was able to predict the evolution of the mechanical integrity of the oxygen carrier particles observed in CLG prototypes that operate with continuous fuel supply. Thus, this study provides a straightforward method to identify promising $\text{Fe}_2\text{O}_3/\text{Al}_2\text{O}_3$ oxygen carriers for use in CLG units, as well as to determine the best operating conditions to preserve the mechanical integrity of the oxygen carrier particles without the need for costly prototype testing.

CRedit authorship contribution statement

Iván Samprón: Conceptualization, Methodology, Validation, Investigation, Resources, Writing – original draft, Visualization. **Francisco García-Labiano:** Writing – review & editing, Writing – original draft, Supervision, Project administration, Methodology, Investigation, Funding acquisition, Data curation, Conceptualization. **María T. Izquierdo:** Conceptualization, Methodology, Writing – review & editing. **Luis F. de Diego:** Writing – review & editing, Writing – original draft, Visualization, Validation, Supervision, Resources, Project administration, Methodology, Funding acquisition, Data curation, Conceptualization.

Declaration of Competing Interest

The authors declare that they have no known competing financial interests or personal relationships that could have appeared to influence the work reported in this paper.

Data availability

Data will be made available on request.

Acknowledgements

This work was supported by the CO2SPLIT Project, Grant PID2020-

113131RB-I00, funded by MICIN/AEI/10.13039/501100011033. I. Samprón thanks the Spanish Ministerio de Ciencia, Innovación y Universidades (MICIU) for the PRE2018-086217 predoctoral fellowship.

Appendix A. Supplementary material

Supplementary data to this article can be found online at <https://doi.org/10.1016/j.fuel.2023.129326>.

References

- [1] Sikarwar VS, Zhao M, Fennell PS, Shah N, Anthony EJ. Progress in biofuel production from gasification. *Progr Energy Combust* 2017;61:189–248.
- [2] IEA 2021. Net zero by 2050. A Roadmap for the Global Energy Sector.
- [3] Ge H, Guo W, Shen L, Song T, Xiao J. Biomass gasification using chemical looping in a 25 kWth reactor with natural hematite as oxygen carrier. *Chem Eng J* 2016; 286:174–83.
- [4] Shen T, Wu J, Shen L, Yan J, Jiang S. Chemical looping gasification of coal in a 5 kWth interconnected fluidized bed with a two-stage fuel reactor. *Energ Fuel* 2018; 32(4):4291–9.
- [5] Condori O, de Diego LF, García-Labiano F, Izquierdo MT, Abad A, Adánez J. Syngas production in a 1.5 kWth biomass chemical looping gasification unit using Fe and Mn ores as the oxygen carrier. *Energ Fuel* 2021;35(21):17182–96.
- [6] Pans MA, Gayán P, de Diego LF, García-Labiano F, Abad A, Adánez J. Performance of a low-cost iron ore as an oxygen carrier for chemical looping combustion of gaseous fuels. *Chem Eng Res Des* 2015;93:736–46.
- [7] Condori O, García-Labiano F, de Diego LF, Izquierdo MT, Abad A, Adánez J. Biomass chemical looping gasification for syngas production using ilmenite as oxygen carrier in a 1.5 kWth unit. *Chem Eng J* 2021;405:126679.
- [8] Condori O, García-Labiano F, de Diego LF, Izquierdo MT, Abad A, Adánez J. Biomass chemical looping gasification for syngas production using LD Slag as oxygen carrier in a 1.5 kWth unit. *Fuel Pro Tech* 2021;222:106963.
- [9] Huang Z, He F, Feng Y, Liu R, Zhao K, Zheng A, et al. Characteristics of biomass gasification using chemical looping with iron ore as an oxygen carrier. *Int J Hydrogen Energy* 2013;38(34):14568–75.
- [10] Huseyin S, Wei G-Q, Li H-B, He F, Huang Z. Chemical-looping gasification of biomass in a 10 kWth interconnected fluidized bed reactor using $\text{Fe}_2\text{O}_3/\text{Al}_2\text{O}_3$ oxygen carrier. *J Fuel Chem Technol* 2014;42(8):922–31.
- [11] Wei G, He F, Huang Z, Zheng A, Zhao K, Li H. Continuous operation of a 10 kWth chemical looping integrated fluidized bed reactor for gasifying biomass using an iron-based oxygen carrier. *Energ Fuel* 2015;29(1):233–41.
- [12] Gayán P, Pans MA, Ortiz M, Abad A, de Diego LF, García-Labiano F, et al. Testing of a highly reactive impregnated $\text{Fe}_2\text{O}_3/\text{Al}_2\text{O}_3$ oxygen carrier for a SR-CLC system in a continuous CLC unit. *Fuel Pro Tech* 2012;96:37–47.
- [13] de Diego LF, García-Labiano F, Gayán P, Abad A, Cabello A, Adánez J, et al. Performance of Cu- and Fe-based oxygen carriers in a 500 Wth CLC unit for sour gas combustion with high H_2S content. *Int J Green Gas Control* 2014;28:168–79.
- [14] García-Labiano F, de Diego LF, Gayán P, Abad A, Cabello A, Adánez J, et al. Energy exploitation of acid gas with high H_2S content by means of a chemical looping combustion system. *App Energy* 2014;136:242–9.
- [15] Serrano A, García-Labiano F, de Diego LF, Gayán P, Abad A, Adánez J. Chemical looping combustion of liquid fossil fuels in a 1 kWth unit using a Fe based oxygen carrier. *Fuel Pro Tech* 2017;160:47–54.
- [16] Cabello A, Dueso C, García-Labiano F, Gayán P, Abad A, de Diego LF, et al. Performance of a highly reactive impregnated $\text{Fe}_2\text{O}_3/\text{Al}_2\text{O}_3$ oxygen carrier with CH_4 and H_2S in a 500 Wth CLC unit. *Fuel* 2014;121:117–25.
- [17] Samprón I, de Diego LF, García-Labiano F, Izquierdo MT, Abad A, Adánez J. Biomass chemical looping gasification of pine wood using a synthetic $\text{Fe}_2\text{O}_3/\text{Al}_2\text{O}_3$ oxygen carrier in a continuous unit. *Bioresource Technol* 2020;316:123908.
- [18] Qin L, Majumder A, Fan JA. Evolution of nanoscale morphology in single and binary metal oxide microparticles during reduction and oxidation processes. *J Mater Chem* 2014;2(41):17511–20.
- [19] Saito Y, Kosaka F, Kiruchi N, Hatano H, Otomo J. Evaluation of microstructural changes and performance degradation in iron-based oxygen carriers during redox cycling for chemical looping systems with image analysis. *Ind Eng Chem Res* 2018; 57(16):5529–38.
- [20] Ma Z, Liu G, Lu Y, Zhang H. Redox performance of $\text{Fe}_2\text{O}_3/\text{Al}_2\text{O}_3$ oxygen carrier calcined at different temperature in chemical looping process. *Fuel* 2022;310: 122381.
- [21] Samprón I, de Diego LF, García-Labiano F, Izquierdo MT. Effect of the Fe content on the behavior of synthetic oxygen carriers in a 1.5 kW biomass chemical looping gasification unit. *Fuel* 2022;309:122193.
- [22] Adánez J, de Diego LF, García-Labiano F, Gayán P, Abad A, Palacios JM. Selection of oxygen carriers for chemical-looping combustion. *Energ Fuel* 2004;18(2): 371–7.
- [23] Cabello A, Abad A, García-Labiano F, Gayán P, de Diego LF, Adánez J. Kinetic determination of a highly reactive impregnated $\text{Fe}_2\text{O}_3/\text{Al}_2\text{O}_3$ oxygen carrier for use in gas fueled chemical looping combustion. *Chem Eng J* 2014;258:265–80.
- [24] Samprón I, de Diego LF, García-Labiano F, Izquierdo MT. Optimization of synthesis gas production in the biomass chemical looping gasification process operating under auto-thermal conditions. *Energ* 2021;226:120317.

- [25] Dieringer P, Marx F, Alobaid F, Ströle J, Epple B. Process control strategies in chemical looping gasification-A novel Process for the production of biofuels allowing for net negative CO2 emissions. *Appl Sci* 2020;10:4271.
- [26] Dieringer P, Marx F, Michel B, Ströhle J, Epple B. Design and control concept of a 1 MWth chemical looping gasifier allowing for efficient autothermal syngas production. *Int J Green Gas Control* 2023;127:103929.
- [27] Condori O, Abad A, Izquierdo MT, de Diego LF, García-Labiano F, Adánez J. Assessment of the chemical looping gasification of wheat straw pellets at the 20 kWth scale. *Fuel* 2023;344:128059.
- [28] Cabello A, Abad A, Mendiara T, Izquierdo MT, de Diego LF. Outstanding performance of a Cu-based oxygen carrier impregnated on alumina in chemical looping combustion. *Chem Eng J* 2023;455:140484.
- [29] Mendiara T, Pérez-Astray A, Izquierdo MT, Abad A, de Diego LF, García-Labiano F, et al. Chemical looping combustion of different types of biomass in a 0.5 kWth unit. *Fuel* 2018;211:868–75.